Poccia, D. L., Simpson, M. V., & Green, G. R. (1987) *Dev. Biol. 121*, 445–453.
Puigdomenech, P., Romero, M. C., Allan, J., Sautiere, P., Giancotti, V., & Crane-Robinson, C. (1987) *Biochim. Biophys. Acta 908*, 70–80.
Rodrigues, J., Brandt, W., & Von Holt, C. (1985) *Eur. J. Biochem. 150*, 499–506.
Savič, A., Richman, P., Williamson, P., & Poccia, D. (1981) *Dev. Biol. 78*, 3706–3710.
Simpson, R. T., & Bergman, L. W. (1982) *J. Biol. Chem. 255*, 10702–10709.
Simpson, M. V., & Poccia, D. L. (1987) *Gamete Res. 17*, 131–144.
Spadafora, C., Bellard, M., Compton, J., & Chambon, P. (1976) *FEBS Lett. 69*, 281–285.
Strickland, M., Strickland, W., Brandt, W., Von Holt, C., Wittman-Liebold, B., & Lehmann, A. (1978) *Eur. J. Biochem. 89*, 443–452.
Strickland, W. N., Strickland, M., Brandt, W. F., Von Holt, C., Lehmann, A., & Wittmann-Liebold, B. (1980) *Eur. J. Biochem. 104*, 567–578.
Von Holt, C., de Groot, P., Schwager, S., & Brandt, W. F. (1984) in *Histone Genes* (Stein, G. S., Stein, J. L., & Marzluff, W. F., Eds.) pp 65–104, Wiley, New York.
Zalenskaya, I., Pospelov, V., Zalensky, A., & Vorob'ev, V. (1981) *Nucleic Acids Res. 9*, 473–487.

Investigations of the Partial Reactions Catalyzed by Pyruvate Phosphate Dikinase†

Hsuei Chin Wang,‡ Lawrence Ciskanik,‡ Debra Dunaway-Mariano,*,‡,§ Wolfgang von der Saal,‖ and Joseph J. Villafranca*,‖

Department of Chemistry and Biochemistry, University of Maryland, College Park, Maryland 20742, and Department of Chemistry, The Pennsylvania State University, University Park, Pennsylvania 16802

Received June 5, 1987; Revised Manuscript Received August 18, 1987

ABSTRACT: The kinetic mechanism of pyruvate phosphate dikinase (PPDK) from *Bacteroides symbiosus* was investigated with several different kinetic diagnostics. Initial velocity patterns were intersecting for AMP/PP_i and ATP/P_i substrate pairs and parallel for all other substrate pairs. PPDK was shown to catalyze [^{14}C]pyruvate ⇄ phosphoenolpyruvate (PEP) exchange in the absence of cosubstrates, [^{14}C]AMP ⇄ ATP exchange in the presence of P_i/PP_i but not in their absence, and [^{32}P]P_i ⇄ PP_i exchange in the presence of ATP/AMP but not in their absence. The enzyme was also shown, by using [$\alpha\beta$-^{18}O,β,β-$^{18}O_2$]ATP and [$\beta\gamma$-^{18}O,γ,γ,γ-$^{18}O_3$]ATP and ^{31}P NMR techniques, to catalyze exchange in ATP between the $\alpha\beta$-bridge oxygen and the α-P nonbridge oxygen and also between the $\beta\gamma$-bridge oxygen and the β-P nonbridge oxygen. The exchanges were catalyzed by PPDK in the presence of P_i but not in its absence. These results were interpreted to support a bi(ATP,P_i) bi(AMP,PP_i) uni(pyruvate) uni(PEP) mechanism. AMP and P_i binding order was examined by carrying out dead-end inhibition studies. The dead-end inhibitor adenosine 5′-monophosphorothioate (AMPS) was found to be competitive vs AMP, noncompetitive vs PP_i, and uncompetitive vs PEP. The dead-end inhibitor imidodiphosphate (PNP) was found to be competitive vs PP_i, uncompetitive vs AMP, and uncompetitive vs PEP. These results showed that AMP binds before PP_i. The ATP and P_i binding order was studied by carrying out inhibition, positional isotope exchange, and alternate substrate studies. The dead-end inhibitor adenylyl imidodiphosphate (AMPPNP) was shown to be noncompetitive vs P_i, which ruled out an ordered mechanism in which P_i binds first. The positional isotope exchange rates observed with [$\alpha\beta$-^{18}O,β,β-$^{18}O_2$]ATP as a function of P_i concentration followed a normal saturation curve, eliminating an ordered mechanism in which ATP binds first. The initial velocities of the PPDK-catalyzed reaction of P_i and of the two alternate substrates arsenate and thiophosphate were measured as a function of ATP concentration. A Lineweaver–Burk plot of these data indicated a random mechanism. Product inhibition studies were carried out by using initial velocity and equilibrium isotope exchange techniques. The results from these studies indicate that the ATP/P_i and AMP/PP_i binding steps are at steady state and that AMP forms an abortive complex. Two possible chemical mechanisms are described, one of which involves the intermediacies of a covalent pyrophosphoryl-enzyme and a covalent phosphoryl-enzyme and the other of which involves the intermediacies of ADP and a covalent phosphoryl-enzyme.

Pyruvate phosphate dikinase (PPDK)[1] catalyzes the reversible phosphorylation of pyruvate and inorganic phosphate by a single molecule of ATP: pyruvate + ATP + P_i ⇄ PEP + AMP + PP_i. The enzyme has been found in the amoeba *Entamoeba histolytica* (Reeves, 1960), in the leaves of C_4 plants (Hatch & Slack, 1968), and in a variety of bacteria (Evans & Wood, 1968; Reeves et al., 1968; Buchanan, 1974;

† This work was supported by NSF Grant PCM-8409737 to J.J.V. and NIH Grants GM 28688 and GM 36260 to D.D.-M.
* Author to whom correspondence should be addressed.
‡ University of Maryland.
§ NIH Career Development Awardee (ES 00111) and Alfred P. Sloan Fellow.
‖ The Pennsylvania State University.

[1] Abbreviations: PPDK, pyruvate phosphate dikinase; PEP, phosphoenolpyruvate; NMR, nuclear magnetic resonance; HPLC, high-pressure liquid chromatography; SDS–PAGE, sodium dodecyl sulfate–polyacrylamide gel electrophoresis; FPLC, fast protein liquid chromatography; TLC, thin-layer chromatography; HEPES, *N*-(2-hydroxyethyl)piperazine-*N*′-2-ethanesulfonic acid; PIPES, piperazine-*N*,*N*′-bis(2-ethanesulfonic acid); EDTA, ethylenediaminetetraacetic acid; AMPS, adenosine 5′-monophosphorothioate; PNP, imidodiphosphate; AMPPNP, adenylyl imidodiphosphate; PIX, positional isotope exchange; Tris, tris(hydroxymethyl)aminomethane; TCA, trichloroacetic acid; AMPPCP, adenylyl methylenediphosphate; AMPCPP, adenosine 5′-(α,β-methylenetriphosphate).

0006-2960/88/0427-0625$01.50/0

Scheme I

$$E^{his} + ATP \rightleftarrows E^{his}\text{–}\overset{\beta\ \gamma}{P}P + AMP \quad (I)$$

$$E^{his}\text{–}\overset{\beta\ \gamma}{P}P + P_i \rightleftarrows E^{his}\text{–}\overset{\beta}{P} + \overset{\gamma}{P}P_i \quad (II)$$

$$E^{his}\text{–}\overset{\beta}{P} + \text{pyruvate} \rightleftarrows E^{his} + \overset{\beta}{P}EP \quad (III)$$

Benziman & Palgi, 1970). The metabolic function of PPDK varies with the type of organism in which it is present. In *Acetobacter xylimum*, in *Propionibacterium shermanii*, and in C_4 plants it functions in the direction of PEP formation while in *Bacteroides symbiosus* and *E. histolytica* where pyruvate kinase is absent, PPDK functions in the direction of ATP synthesis.

Previous studies of the amoeba and bacterial dikinases have shown that the overall reaction involves three phosphoryl-transfer steps which culminate in the transfer of the γ-phosphoryl of ATP to P_i and the transfer of the β-phosphoryl of ATP to pyruvate (Evans & Wood, 1968; Reeves et al., 1960). Recent stereochemical studies carried out by Cook and Knowles (1985) have shown that the γ-phosphoryl group of ATP undergoes a single displacement during the course of its transfer to P_i while the β-phosphoryl group undergoes two displacement reactions during its transfer to pyruvate. These results are consistent with the reaction mechanism previously proposed for the *P. shermanii* enzyme (Milner & Wood, 1976) and for the *B. symbiosus* enzyme (Milner et al., 1978). According to this mechanism an active site histidine residue is pyrophosphorylated by ATP (Goss et al., 1980; Spronk et al., 1976; Phillips & Wood, 1986). The pyrophosphorylated histidine residue migrates to a second reaction site where the terminal phosphoryl group is transferred to P_i. The phosphorylated histidine residue then migrates to a third site where the phosphoryl group is transferred to pyruvate. The three partial reactions of this nonclassical tri uni uni mechanism are illustrated in Scheme I. Our own investigations of the *B. symbiosus* enzyme have required us to repeat and extend many of the original kinetic studies. The results from our studies are described in this paper and are interpreted as evidence against the tri uni uni mechanism and in support of a bi-(ATP,P_i) bi(AMP,PP_i) uni(pyruvate) uni(PEP) kinetic mechanism. Furthermore, the consequence of our findings in relation to the consideration of possible chemical mechanisms of the catalyzed reaction is described.

Experimental Procedures

PPDK Purification. PPDK was purified from *B. symbiosus* obtained from the American Type Culture Center (14940) and from *B. symbiosus* that was kindly provided by Drs. Nelson Phillips and Harland Wood of the Department of Biochemistry, Case Western Reserve School of Medicine. The enzyme was purified in essentially the same manner as described by Goss et al. (1980) with the exception of the addition of a final chromatographic step involving (Pharmacia) Superose-6 FPLC chromatography. This step was necessary to remove a protein contaminant that was present in the amount of 10–30% of the protein of the final PPDK preparation. This contaminant displayed both PPDK and myokinase activities. Elution of the PPDK from the column was accomplished with 14–15 mL of a pH 6.5 buffer containing 20 mM imidazole, 0.1 mM EDTA, 0.7 mM 2-mercaptoethanol, and 100 mM KCl (flow rate = 0.4 mL/min). The protein contaminant eluted with 16–17 mL of buffer.[2] The PPDK prepared in this manner migrated as a single protein band on PAGE gels (5% polyacrylamide; 5 mM Tris/38 mM glycine, pH 8.3, running buffer) and on SDS–PAGE gels. The specific activity of the "pure" enzyme varied from preparation to preparation and ranged from 10 to 24 units/mg.

PPDK Reaction Assays. The overall reaction was monitored in the reverse direction (ATP forming) at 340 nm by using the lactate dehydrogenase (10 units/mL)–NADH (0.4 mM) coupling reaction. The forward reaction (AMP forming) was driven to completion with yeast inorganic pyrophosphatase. Reaction progress was monitored by carrying out the reaction with ^{14}C-labeled ATP, separating the ATP and AMP with silica gel TLC [2-propanol/H_2O/14.5 M NH_4OH (7:2:1) solvent], and determining the ratio of [^{14}C]ATP and [^{14}C]-AMP with a liquid scintillation counter. The exchange reactions ([^{14}C]AMP $\rightleftarrows$ ATP; [^{32}P]P_i $\rightleftarrows$ PP_i; [^{14}C]pyruvate $\rightleftarrows$ PEP) were monitored by chromatographic separation of the species undergoing exchange and quantitation of their radiolabel by liquid scintillation counting. The ATP and AMP were separated by using either silica gel TLC (vide supra) or anion-exchange HPLC [4.6 mm × 25 cm Ultrasil AX column; 0.5 M phosphate buffer (pH 3.5) eluant; 1 mL/min flow rate]. The P_i and PP_i were separated with cellulose TLC [2-propanol/20% TCA/30% NH_4OH (72:25:0.25) solvent; Hanes–Isherwood spray developer (Hanes & Isherwood, 1949)]. The PEP and pyruvate were separated with cellulose TLC plates and methanol/H_2O (85:15) solvent. The exchange of [^{14}C]AMP into AMPPNP and AMPPCP was tested by using silica gel TLC [2-propanol/H_2O/14.5M NH_4OH (7:2:1) solvent]. All reactions were carried out at 25 °C.

Velocity Data Analysis. The initial velocity data obtained from kinetic experiments in which the concentrations of two of the three substrates were varied while the third was held constant were first analyzed by constructing Lineweaver–Burk plots. Equations 1 and 2a were employed to computer fit data (Cleland, 1979) for which the double-reciprocal plots conformed respectively to an intersecting initial velocity pattern and a parallel initial velocity pattern; in these equations, v =

$$v = \frac{VAB}{K_{ia}K_b + K_aB + K_bA + AB} \quad (1)$$

$$v = \frac{VAB}{K_aB + K_bA + AB} \quad (2a)$$

initial velocity, V = maximal velocity, A = concentration of substrate A, B = concentration of substrate B, K_a = Michaelis constant for substrate A, K_b = Michaelis constant for substrate B, and K_{ia} = dissociation constant for substrate A.

The initial velocity data obtained from the dead-end inhibitor and product inhibition studies were first analyzed by constructing Lineweaver–Burk plots. Equations 2b, 3, and 4 were employed to computer fit (Cleland, 1979) data for which the double-reciprocal plots conformed respectively to linear competitive inhibition, linear uncompetitive inhibition, and linear noncompetitive inhibition; in these equations, K_{is} = slope

[2] We briefly investigated the origin and nature of this protein. First, the protein was found to migrate as two protein bands (which were stained by Coomassie blue with equal intensity) on the PAGE gel and SDS–PAGE gel. One of the protein species comigrated with native PPDK, and the other migrated faster. The species that comigrated with native PPDK was eluted from the PAGE gel and found to possess normal PPDK activity and no myokinase activity. The approximate molecular mass of the faster migrating species was judged to be ca. 30 000 daltons. This species was isolated from the PAGE gel and shown to possess myokinase activity (ca. 1 unit/mg at pH 6.9) and no PPDK activity.

$$v = \frac{VA}{K_a(1 + I/K_{is}) + A} \quad (2b)$$

$$v = \frac{VA}{K_a + (1 + I/K_{ii})A} \quad (3)$$

$$v = \frac{VA}{K_a(1 + I/K_{is}) + (1 + I/K_{ii})A} \quad (4)$$

inhibition constant, K_{ii} = intercept inhibition constant, and I = inhibitor concentration. The velocities of the exchange reactions were calculated from plots of ln $(1 - f)$ vs time with eq 5 (Boyer, 1959), where a = concentration of radiolabeled

$$-\ln(1 - f) = V_{ex}\frac{(a + b)t}{ab} \quad (5)$$

exchanging substrate, b = concentration of nonlabeled exchanging substrate, and f = ratio of the specific activity of b at time t and at $t = \infty$. The exchange velocities obtained in this manner were divided by the maximum velocity of the overall reaction measured in the forward (slow) direction to yield the V_{ex}/V_{cat} values reported in Table II.

Positional Isotope Exchange Experiments (PIX). ^{18}O-Labeled ATP. The labeled nucleotide [$\alpha\beta$-^{18}O,β,β-$^{18}O_2$]ATP (**1**) was prepared in 20% yield (90–95 atom % ^{18}O in the three positions) in the following manner. Adenosine 5′-(4-morpholino)phosphate (Moffatt & Khorana, 1961) (156 mg; 200 μmol) was dried by four evaporations with 2 mL of dry pyridine. A mixture of 600 μL of 1.0 M $H_3P^{18}O_4$ (600 μmol) and 150 μL (600 μmol) of tributylamine was dried in the same manner. The residue was dissolved in 6 mL of dry dimethyl sulfoxide and combined with the morpholidate. Six milliliters of water was added to the reaction mixture after it had incubated at 35 °C for 20 h. The resulting solution was chromatographed on a 5 × 30 cm DEAE-cellulose column using a linear gradient of triethylammonium bicarbonate buffer, pH 7.6 (4 L, 0.05–0.5 M). The [$\alpha\beta$-^{18}O,β,β,β-$^{18}O_3$]ADP (eluted at 0.3 M buffer) containing fractions were pooled and concentrated in vacuo. Conversion of this compound to [$\alpha\beta$-^{18}O,β,β-$^{18}O_2$]ATP was carried out according to literature procedures (Midelfort & Rose, 1976). [$\beta\gamma$-^{18}O,γ,γ,γ-$^{18}O_3$]-ATP (**5**) was prepared according to the method of Midelfort and Rose (1976). The ^{31}P NMR signals of **5** showed that the ratio of $P^{18}O_4$:$PO^{18}O_3$ was 80:20, which corresponds to ca. 95 atom % ^{18}O in each of the four positions.

PIX Reactions. One-milliliter solutions containing the substrates and metal ions were equilibrated at 30 °C for 10 min. The reactions were started by the addition of enzyme and stopped by the addition of 0.5 mL of 0.2 M EDTA in 1 M Tris buffer (pH 8.5) and a few drops of CCl_4. After the reactions were vigorously vortexed and centrifuged to remove protein, 0.4 mL of D_2O was added to the solution. ^{31}P NMR (Cohn & Hu, 1978) was used to observe and quantitate the different isotopically labeled species present in the solution. The proton-decoupled ^{31}P NMR spectra were taken at 145.81 MHz on a Bruker WM 360 spectrometer using a 5-kHz sweep width. A total of 2000 scans were accumulated with an acquisition time of 1.64 s. To improve the digital resolution, zero filling to 64K was applied prior to Fourier transformation.

Results

Substrate Initial Velocity Studies. Initial velocity patterns were constructed by plotting the inverse of the initial reaction velocity measured at varying fixed levels of one substrate vs the inverse of the concentration of the second substrate (the concentration of the third substrate was held constant). We first examined the initial velocity patterns for the reverse reaction (ATP forming) so that we could use the convenient LDH/NADH coupled spectrophotometric assay. The patterns arising from variation of the concentration of AMP and PP_i (PEP saturating) were intersecting while patterns arising from variation of the concentration of AMP and PEP (PP_i nonsaturating) or PP_i and PEP (AMP nonsaturating) were parallel. The intersecting patterns observed for the AMP/PP_i pair indicate that AMP and PP_i bind to enzyme forms that are reversibly connected. The parallel patterns observed for the AMP/PEP and PP_i/PEP pairs, on the other hand, indicate that PEP binds to an enzyme form that is not reverisbly connected to those enzyme forms that bind AMP and PP_i. To check for reversible connection between the enzyme forms that bind ATP and P_i, we examined the ATP/P_i (pyruvate nonsaturating) patterns. These patterns are intersecting, indicating reversible connection. The kinetic constants calculated from the initial velocity data are summarized in Table I.

Isotope Exchange Studies. The results from the substrate initial velocity studies suggested a bi bi uni uni mechanism for the forward reaction (AMP forming). We tested this mechanism further by testing the cosubstrate requirement for PPDK catalysis of the three isotope exchange reactions: [^{14}C]AMP $\rightleftarrows$ ATP; [^{32}P]P_i $\rightleftarrows$ PP_i; [^{14}C]pyruvate $\rightleftarrows$ PEP. The rates of the exchange reactions were measured under three different sets of conditions: (1) enzyme plus cofactors, (2) enzyme, cofactors, and one cosubstrate/product pair, and (3) enzyme, cofactors, and both cosubstrate/product pairs. The rate data obtained are shown in Figure 1, and the exchange velocities calculated from these data are summarized in Table II. Only the [^{14}C]pyruvate $\rightleftarrows$ PEP exchange reaction takes place at an appreciable rate in the absence of added cosubstrates. The P_i/PP_i pair were required for [^{14}C]AMP $\rightleftarrows$ ATP exchange, and the AMP/ATP pair were required for the [^{32}P]P_i $\rightleftarrows$ PP_i exchange.[3]

PIX Studies. According to the PPDK reaction mechanism proposed by Wood and co-workers (see Scheme I) cleavage of the ATP between the α- and β-P (partial reaction I) should take place in the absence of P_i while cleavage at the $\beta\gamma$-position (partial reaction II) should require the participation of P_i. The results from the initial velocity and equilibrium isotope studies reported above indicate that P_i is required for partial reaction I as well as II. However, these results do not distinguish between P_i requirement for AMP formation on the enzyme and P_i requirement for release of AMP from the enzyme. In order to make this distinction, we tested the P_i dependency of the α,β-P and β,γ-P cleavage reactions by testing the ability of PPDK to catalyze positional isotope exchange (PIX) in [$\alpha\beta$-^{18}O,β,β-$^{18}O_2$]ATP (**1**) and [$\beta\gamma$-^{18}O,γ,γ,γ-$^{18}O_3$]ATP (**5**).[4] As indicated in Scheme II, reversible α,β-P cleavage accompanied by torsional equilibration of the AMP α-P oxygen atoms will lead to the formation of [α-^{18}O,β,β-$^{18}O_2$]ATP (**2**). If β,γ-P cleavage follows (as would be expected if P_i were present), [$\beta\gamma$-^{18}O,β-^{18}O,$\alpha\beta$-^{18}O]ATP (**3**) and [$\beta\gamma$-^{18}O,β-^{18}O,α-^{18}O]ATP (**4**) may also be formed. Positional isotope exchange in [$\beta\gamma$-^{18}O,γ,γ,γ-$^{18}O_3$]ATP (**5**) can only take place if reversible cleavage of the β,γ-P position takes place. Ac-

[3] The $V_{ex}/V_{cat} < 1$ for these two exchange reactions. We attribute this inequality to product inhibiton.

[4] This approach is not free of ambiguity. In particular, it is perhaps possible that enzyme-bound P_i may somehow be required to allow for torsional equilibration of the α-P oxygen atoms of the enzyme-bound AMP. Thus, P_i would not only be necessary for AMP release (molecular isotope exchange) but also AMP $C_{5'}$–O–P bond rotation (PIX).

Table I: Apparent Kinetic Constants for PPDK Determined from Initial Velocity Studies[a]

varied substrate	changing fixed substrate	obsd pattern	app K_m (mM)	app K_i (mM)	fixed substrate[b]
AMP	PP_i	intersecting	0.121 ± 0.008	0.20 ± 0.003	PEP
	PEP	parallel	0.020 ± 0.002		PP_i
PP_i	AMP	intersecting	0.017 ± 0.001	0.028 ± 0.003	PEP
	PEP	parallel	0.06 ± 0.02		AMP
PEP	AMP	parallel	0.036 ± 0.008		PP_i
	PP_i	parallel	0.10 ± 0.02		AMP
ATP	P_i	intersecting	0.004 ± 0.0004	0.030 ± 0.003	pyruvate
P_i	ATP	intersecting	0.30 ± 0.02	2.0 ± 0.3	pyruvate

[a] All reactions contained 3.5 mM $MgCl_2$, 20 mM NH_4Cl, and 60 mM PIPES (pH 6.9). [b] Concentrations were PEP, 2.0 mM; PP_i, 0.06 mM; AMP, 0.05 mM; and pyruvate, 0.5 mM.

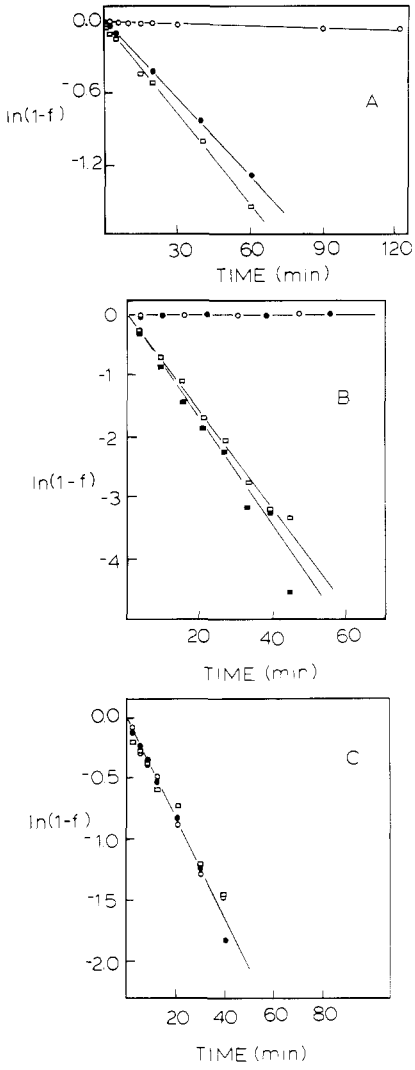

FIGURE 1: Equilibrium isotope exchange kinetics of the partial reactions catalyzed by PPDK. The experimental conditions are described in Table II. (A) [^{14}C]AMP ⇄ ATP exchange: (○) no added substrates, (●) P_i and PP_i added, and (□) P_i, PP_i, PEP, and pyruvate added. (B) [^{32}P]P_i ⇄ PP_i exchange: (○) no added substrate, (●) PEP and pyruvate added, (□) AMP and ATP added, and (■) AMP, ATP, PEP, and pyruvate added. (C) [^{14}C]Pyruvate ⇄ PEP exchange: (○) no added cosubstrates, (●) P_i and PP_i added, and (□) AMP, ATP, P_i, and PP_i added.

cordingly, **5** should be converted to [β-^{18}O,γ,γ,γ-^{18}O$_3$]ATP (**6**) (Scheme III).

The conversions of **1** to **2**, **3**, and **4** and of **5** to **6** were monitored by ^{31}P NMR. Shown in Figures 2 and 3 are the ^{31}P NMR spectra of the [$\alpha\beta$-^{18}O,β,β-^{18}O$_2$]ATP (**1**) and the [$\beta\gamma$-^{18}O,γ,γ,γ-^{18}O$_3$]ATP (**5**) reaction mixtures prior to and after the addition of P_i and PPDK. The ^{31}P NMR spectrum of our preparation of **1** (Figure 2A) revealed that ca. 70% of the nucleotide was actually [$\alpha\beta$-^{18}O,β,β-^{18}O$_2$]ATP while the

Scheme II: Products Expected from PPDK-Catalyzed PIX of [$\alpha\beta$-^{18}O,β,β-^{18}O$_2$]ATP (**1**)[a]

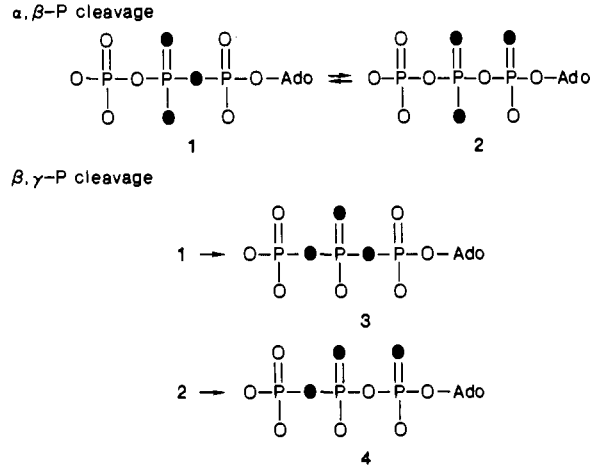

[a] O = ^{16}O and ● = ^{18}O.

Scheme III: Product Expected from PIX of [$\beta\gamma$-^{18}O,γ,γ,γ-^{18}O$_3$]ATP (**5**)

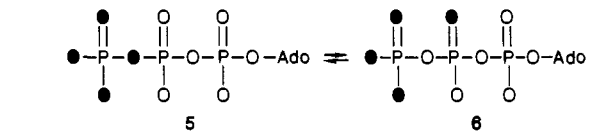

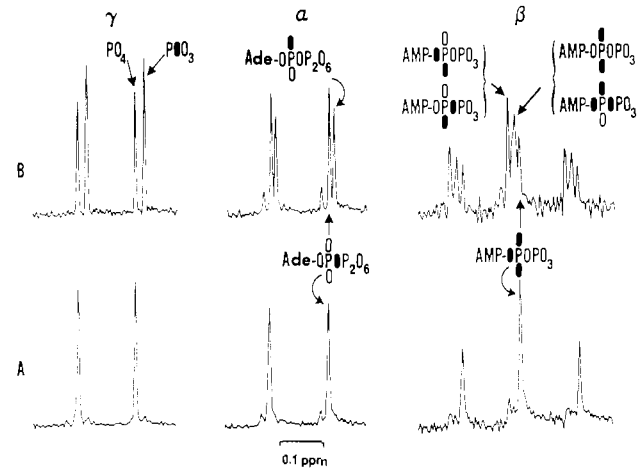

FIGURE 2: ^{31}P NMR spectrum at 145.81 MHz of (A) [$\alpha\beta$-^{18}O,β,β-^{18}O$_2$]ATP (**1**) and (B) PIX reaction mixture of **1** generated from incubation of 230 μg/mL PPDK with 5 mM **1**, 12 mM P_i, 10 mM $MgCl_2$, 20 mM NH_4Cl, and 100 mM imidazole (pH 7.0) at 30 °C for 90 min.

remainder consisted of [$\alpha\beta$-^{18}O,β-^{18}O]ATP (ca. 20%) and [β,β-^{18}O$_2$]ATP (ca. 10%). The $\alpha\beta \rightarrow \alpha$ and $\beta \rightarrow \beta\gamma$ PIX reactions of **1** are evident from the ^{31}P NMR spectrum shown in Figure 2B. Equilibration of [$\alpha\beta$-^{18}O,β,β-^{18}O$_2$]ATP should partition ^{18}O between the $\alpha\beta$-bridge and α-nonbridge positions

Table II: Equilibrium Isotope Exchange Rates Catalyzed by PPDK

[^{14}C]AMP ⇄ ATP		[^{32}P]P_i ⇄ PP_i		[^{14}C]pyruvate ⇄ PEP	
system	V_{ex}/V_{cat}	system	V_{ex}/V_{cat}	system	V_{ex}/V_{cat}
complete[a]	0.001	complete[b]	0.000	complete[c]	1.7
complete[a] + 14 mM P_i and 0.25 mM PP_i	0.20	complete[b] + 0.5 mM AMP and 6 mM ATP	0.06	complete[c] + 10 mM P_i and 1 mM PP	1.7
complete[a] + 8 mM pyruvate and 0.25 mM PEP	0.007	complete[b] + 0.5 mM PEP and 5 mM pyruvate	0.000	complete[c] + 10 mM P_i, 1 mM PP_i, 6 mM ATP, and 0.5 mM AMP	1.7
complete[a] + 14 mM P_i, 0.25 mM PP_i, 8 mM pyruvate, and 0.25 mM PEP	0.25	complete[b] + 0.5 mM AMP, 6 mM ATP, 0.5 mM PEP, and 5 mM pyruvate	0.06		

[a] Complete system contains 1–10 units/mL PDK, 15 mM $MgCl_2$, 100 mM NH_4Cl, 150 mM imidazole (pH 6.9), 0.5 mM AMP, and 0.5 mM ATP. [b] Complete system contains 1–10 units/mL PPDK, 15 mM $MgCl_2$, 100 mM NH_4Cl, 150 mM imidazole (pH 6.9), 4 mM P_i, and 2 mM PP_i. [c] Complete system contains 1–10 units/mL PPDK, 15 mM $MgCl_2$, 100 mM NH_4Cl, 150 mM imidazole (pH 6.9), 5 mM PEP, and 5 mM pyruvate.

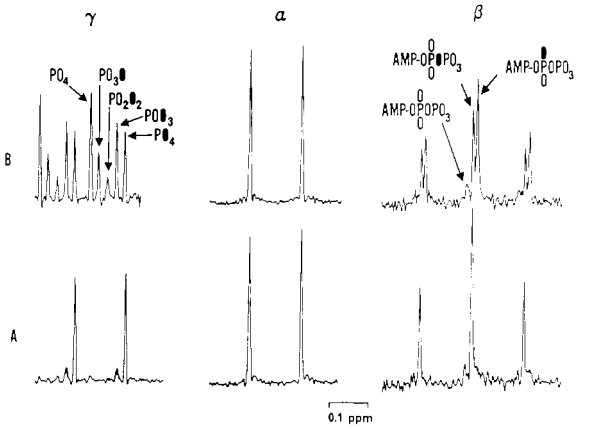

FIGURE 3: ^{31}P NMR spectrum of (A) [$\beta\gamma$-^{18}O,γ,γ,γ-^{18}O$_3$]ATP (**5**) and (B) PIX reaction mixture of **5** generated from incubation of 230 μg/mL PPDK with 5 mM **5**, 12 mM P_i, 10 mM $MgCl_2$, 20 mM NH_4Cl, and 100 mM imidazole (pH 7.0) at 30 °C for 90 min.

in a 1:2 ratio and between the β-nonbridge position and $\beta\gamma$-bridge position in a 1:2 ratio. We calculated these ratios from the ^{31}P NMR spectrum of the PIX reactions of **1** at equilibrium (data not shown) taking into account the presence of the [^{18}O$_2$]ATP contaminants. Both ratios were determined to be 1.0:1.8, close to the theoretical values.

The ^{31}P NMR spectrum of our preparation of **5** (Figure 3A) revealed that 7% of the ATP present contained ^{16}O rather than ^{18}O in the β,γ-P bridge position. This material was also present in the equilibrium mixture (Figure 3B). The remainder of the ATP in the equilibrium mixture had ^{18}O present either in the β,γ-P bridge position (31% of the total ATP) or in the β-P nonbridge position (62% of the total ATP). The ATP that had ^{18}O in the β,γ-P bridge position consisted of **5** and [$\beta\gamma$-^{18}O]-ATP while the ATP that had ^{18}O in the β-P nonbridge position consisted of **6** and [β-^{18}O]ATP. The [$\beta\gamma$-^{18}O]ATP and [β-^{18}O]ATP are formed as a result of the rotation (presumably while dissociated from the enzyme) of the PP_i formed from **5** or **6** followed by transfer of the ^{16}O$_3$ phosphoryl moiety of the PP_i during the back-reaction. As expected, formation of ^{18}O-labeled P_i accompanied the formation of the [β-^{18}O]-ATP and [$\beta\gamma$-^{18}O]ATP.

Next, we examined the dependency of the PIX rates (viz., $\alpha\beta$-^{18}O → α-^{18}O and β-^{18}O → $\beta\gamma$-^{18}O) of **1** on the presence of cosubstrates (see Table III). Addition of P_i to the reaction mixture increased both exchange rates equally, increasing them to 4% of the maximum velocity of the forward (AMP-forming) reaction. In view of the ^{18}O washout that was observed with the [$\beta\gamma$-^{18}O,γ,γ,γ-^{18}O$_3$]ATP (**5**) the slow PIX rate of **1** is probably due to PP_i release from the enzyme and subsequent rebinding. Not surprisingly, the inclusion of PP_i in the reaction increased the PIX rate tenfold by providing a pathway to recycle the phosphorylated enzyme back to free enzyme. Likewise, inclusion of yeast inorganic pyrophosphatase in the reaction prevented the PIX by destroying all PP_i released from the enzyme and thereby drawing all of the enzyme into the phosphorylated form. The addition of 1.6 mM AMP to the PIX reaction to replace the AMP released from the enzyme actually inhibited rather than stimulated the reaction. It was later discovered from the product inhibition studies that this amount of AMP interferes with ATP binding, and thus, we expect that it would also inhibit the PIX rate.

Table III: Rates of PPDK-Catalyzed Positional Isotope Exchange of [$\alpha\beta$-^{18}O,β,β-^{18}O$_2$]ATP (**1**)[a]

enzyme (μg)	ATP (**1**) (mM)	P_i (mM)	PP_i (mM)	AMP (mM)	$\alpha\beta$-^{18}O V_{PIX}/V_{cat} → α-^{18}O (**1** → **2**)	β-^{18}O V_{PIX}/V_{cat} → $\beta\gamma$-^{18}O (**1** → **3**; **2** → **4**)
0	2.0	10	1	0	0.00	0.00
40	2.0	0	0	0	0.00	0.00
40	2.0	10	0	0	0.04	0.04
40	2.0	10	1	0	0.55	0.50
40[b]	2.0	10	0	0	0.00	0.00
20	1.6	10	1	0	0.82	0.86
20[c]	1.6	10	1	1.6	0.36	0.41

[a] The 1-mL reaction solutions contained 10 mM KCl, 10 mM $MgCl_2$, and 100 mM imidazole (pH 7.0). [b] 10 units of yeast inorganic pyrophosphatase were present. [c] The ATP ⇄ AMP molecular exchange rate measured under the same conditions by ^{31}P NMR was V_{ex}/V_{cat} = 0.2.

Substrate Binding Order. The PIX experiments described above support a bi bi uni uni mechanism in which ATP and P_i must be bound to PPDK before AMP formation can take place and in which AMP and PP_i must be bound to the phosphorylated form of the enzyme for P_i formation. We next investigated the order in which the ATP/P_i and AMP/PP_i substrate pairs bind to the enzyme. In the case of the AMP/PP_i pair this was accomplished by carrying out dead-end inhibition studies. Imididodiphosphate (PNP) was utilized as a competitive inhibitor vs PP_i and adenosine 5′-monophosphorothioate (AMPS) was used as a competitive inhibitor vs AMP. The inhibition patterns that are predicted on the basis of random and ordered kinetic mechanisms are listed in Table IV alongside the observed kinetic patterns. These data suggest that AMP binds to the phosphorylated enzyme before PP_i does.

ATP/P_i binding was first examined by measuring the rate at which [$\alpha\beta$-^{18}O,β,β-^{18}O$_2$]ATP (**1**) undergoes PIX as a function of the concentration of P_i present in the PIX reaction mixture. The data obtained and shown in Figure 4 adhere to a normal substrate-saturation curve. This result shows that release of ATP from the central complex (E·ATP·P_i) may precede the release of P_i and thereby rules out a strictly ordered

Table IV: PPDK Dead-End Inhibition Data[a]

		predicted pattern[b]			obsd pattern		
			ordered				
inhibitor	varied substrate	random	AMP (first)	PP_i (first)		K_{is} (mM)	K_{ii} (mM)
AMPS	AMP	C	C	C	C	0.26 ± 0.09	
AMPS	PP	NC	NC	UC	NC	0.7 ± 0.1	2.0 ± 0.2
AMPS	PEP	UC	UC	UC	UC		0.80 ± 0.04
PNP	PP	C	C	C	C	0.25 ± 0.02	
PNP	PEP	UC	UC	UC	UC		0.90 ± 0.05
PNP	AMP	NC	UC	NC	UC		0.62 ± 0.05
		predicted pattern[b]			obsd patttern		
			ordered				
inhibitor	varied substrate	random	ATP (first)	P_i (first)		K_{is} (mM)	K_{ii} (mM)
AMPPNP	ATP	C	C	C	C	0.24 ± 0.02	
AMPPNP	P_i	NC	NC	UC	NC	0.036 ± 0.006	0.11 ± 0.03

[a] Fixed substrates: P_i (0.5 mM), PP_i (0.05 mM), and PEP (0.05 mM) and AMP (0.05 mM) *or* ATP (0.08 mM) and pyruvate (0.05 mM). All reactions contained 10 mM $MgCl_2$, 20 mM NH_4Cl, and 70 mM PIPES (pH 7.0). [b] Competitive inhibition (C), noncompetitive inhibition (NC), and uncompetitive inhibition (UC).

Table V: PPDK Product Inhibition Data[a]

product inhibitor	varied substrate	cosubstrates (mM)	obsd pattern[b]	K_{is} (mM)	K_{ii} (mM)
AMP	ATP	P_i (0.5), pyruvate (0.1)	NC	0.012 ± 0.006	0.05 ± 0.02
AMP	P_i	ATP (0.015), pyruvate (0.1)	NC	0.10 ± 0.05	0.020 ± 0.004
PP_i	ATP	P_i (0.5), pyruvate (0.1)	NC	0.04 ± 0.01	0.10 ± 0.08
PP_i	P_i	ATP (0.015), pyruvate (0.1)	NC	0.05 ± 0.01	0.050 ± 0.008
ATP	AMP	PP_i (0.05), PEP (0.05)	NC	0.22 ± 0.02	1.7 ± 0.1
ATP	PP_i	PP_i (0.05), PEP (0.05)	NC	0.42 ± 0.05	1.50 ± 0.02
ATP	PEP	PP_i (0.05), AMP (0.05)	NC	0.46 ± 0.08	1.5 ± 0.2
P_i	AMP	PP_i (0.05), PEP (0.05)	NC	3.5 ± 0.8	6.3 ± 0.6
P_i	PP_i	AMP (0.05), PEP (0.05)	NC	5 ± 3	11 ± 4

[a] Reactions contained 10 mM $MgCl_2$, 20 mM NH_4Cl, and 75 mM imidazole (pH 6.9) or 75 mM K^+PIPES (pH 7.0). Reactions run in the forward direction (AMP forming) also contained 1 unit/mL yeast inorganic pyrophosphatase with the exception of those reactions in which PP_i was used as product inhibitor. These reactions contained 5 units/mL pyruvate kinase and 0.1 mM ADP. [b] Noncompetitive inhibition (NC).

mechanism in which P_i binds to PPDK after ATP does. Next, we tested the ATP analogue adenyl imidodiphosphate (AMPPNP) as an inhibitor vs P_i. As indicated in Table IV, noncompetitive inhibition was observed. This result eliminates a strictly ordered mechanism in which P_i binds to the enzyme before ATP binds. In order to show that ATP can bind to the free enzyme by this method, we needed a suitable P_i analogue to test as inhibitor vs ATP. Although we were unable to discover a suitable dead-end inhibitor for this purpose, we did succeed in identifying two P_i analogues which serve as alternate substrates for P_i, namely, arsenate and thiophosphate. The availability of these alternate substrates allowed us to further test the ATP/P_i binding order by using the alternate substrate kinetic technique described by Radika and Northrop (1984). The concentration of ATP was varied against fixed, saturating concentrations of P_i, thiophosphate, or arsenate. Reactions contained various amounts of ATP (5–100 μM), 0.5 mM pyruvate, 5 mM $MgCl_2$, 20 mM NH_4Cl, 60 mM PIPES (pH 6.9), and 14 mM P_i (K_m^{app} = 0.7 mM), 20 mM thiophosphate (K_m^{app} = 1.2 mM), or 10 mM arsenate (K_m^{app} = 0.5 mM). The initial velocity data were used to construct a double-reciprocal plot. The K_m and V_{max} values evaluated form this plot are 12.0 μM and 19.1 μM/min (phosphate); 13.2 μM and 13.8 μM/min (arsenate); and 30.0 μM and 14.9 μM/min (thiophosphate). The observed change in the V/K for the reaction of ATP as a result of the change in the cosubstrate suggests that ATP/P_i binding is random.

Product Inhibition Studies. Product inhibition studies were carried out to test for rapid equilibrium binding steps and for abortive complex formation. Product inhibition was tested by measuring the initial velocity of the PPDK-catalyzed reaction at varying concentrations of one substrate and constant subsaturating concentrations of the other two substrates. Reactions contained no product or a fixed level of product which was present at ca. K_i, $2K_i$, or $3K_i$ levels. The results from these experiments are summarized in Table V and interpreted below. Product inhibition was also tested (in the absence of PEP/pyruvate) by measuring the rate of PPDK-catalyzed exchange between [^{14}C]ATP and AMP and between [^{32}P]PP_i and P_i in the presence of the P_i/PP_i pair and the ATP/AMP pair, respectively. The concentrations of two of the reactants were fixed at subsaturating levels while the concentrations of the other two reactants were varied in constant ratio over a wide concentration range. The results obtained from these experiments are depicted in Figure 5 and interpreted below.

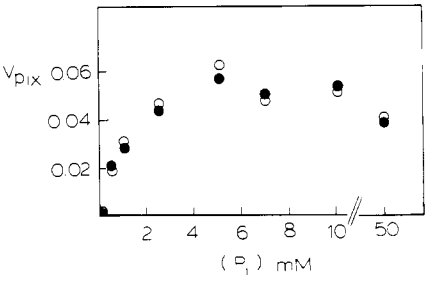

FIGURE 4: Positional isotope exchange of ^{18}O from the $\alpha\beta$-bridge into the α-nonbridge position (○) and from the β-nonbridge position into the $\beta\gamma$-bridge position (●) of [$\alpha\beta$-$^{18}O_3$,β,β-$^{18}O_2$]ATP (**1**). One-milliliter solutions containing 1.5 mM [$\alpha\beta$-$^{18}O_3$,β,β-$^{18}O_2$]ATP, 10 mM KCl, 20 mM $MgCl_2$, 1 mM PP_i, and varying amounts of P_i in 100 mM imidazole buffer, pH 7.0, were incubated in the presence of 20 μg of PPDK at 30 °C for 60 min. The exchange rates were determined from the ^{31}P NMR spectra. V_{PIX} is expressed as μmol/min.

Exchange Reactions of Substrate Analogues. The ATP analogues AMPPNP, AMPPCP, and AMPCPP and the P_i analogue methylenephosphonate were used in isotope exchange experiments for the pupose of determining the order in which

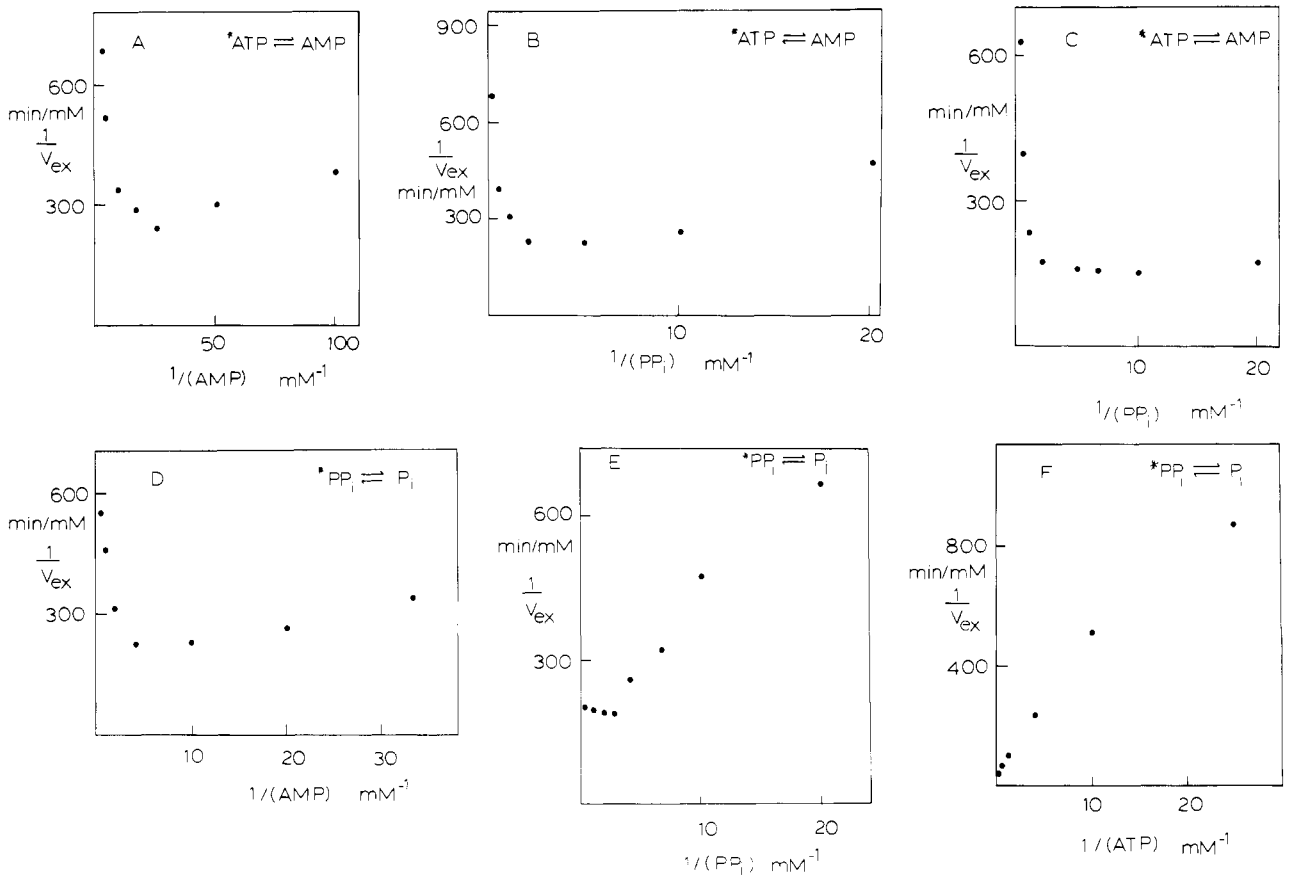

FIGURE 5: PPDK-catalyzed equilibrium isotope exchange. All reactions contained 10 mM $MgCl_2$, 50 mM NH_4Cl, and 75 mM imidazole (pH 6.9). (A) 0.05 mM PP_i, 0.01 mM [^{14}C]ATP, and 0.75–30.0 mM P_i and 0.05–3.0 mM AMP varied in constant ratio. (B) 0.05 mM AMP, 1.0 mM P_i, and 0.005–1.0 mM [^{14}C]ATP and 0.05–10 mM PP_i varied in constant ratio. (C) 0.01 mM [^{14}C]ATP, 0.04 mM AMP, and 0.2–16.0 mM P_i and 0.05–4.0 mM PP_i varied in constant ratio. (D) 0.01 mM ATP, 0.05 mM [^{32}P]PP_i, and 0.3–20.0 mM P_i and 0.03–2.0 mM AMP varied in constant ratio. (E) 0.01 mM ATP, 0.05 mM AMP, and 0.30–30.0 mM P_i and 0.06–6.0 mM [^{32}P]PP_i varied in constant ratio. (F) 1.0 mM P_i, 0.05 mM AMP, and 0.04–5.0 mM ATP and 0.02–2.5 mM [^{32}P]PP_i varied in constant ratio.

Scheme IV

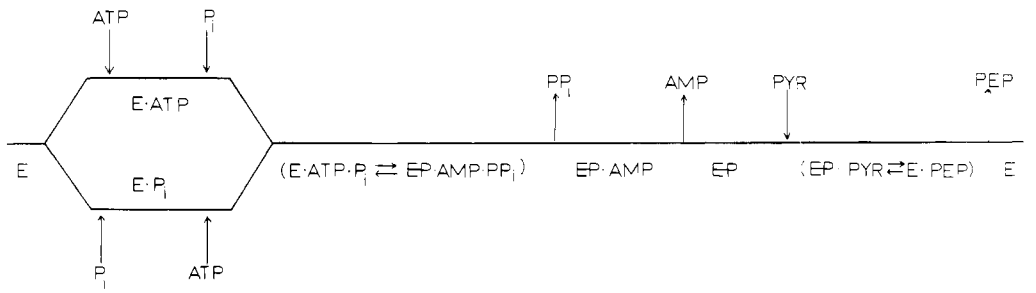

PPDK catalyzes cleavage of the β,γ and α,β bonds in ATP. The [^{14}C]AMP ⇄ AMPPNP and [^{14}C]AMP ⇄ AMPPCP exchange reactions contained 1 mM AMPPNP or AMPPCP, 1 mM [^{14}C]AMP, 2 units/mL PPDK, 20 mM P_i, 1 mM PP_i, 20 mM $MgCl_2$, 100 mM NH_4Cl, and 100 mM imidazole (pH 6.9). After an incubation period of 4 h a detectable level of [^{14}C]AMPPNP or [^{14}C]AMPPCP had not formed in the respective reaction mixtures. The [^{32}P]P_i ⇄ PP_i (AMP/AMPCPP) exchange reaction contained 2 units/mL PPDK, 1 mM [^{32}]P_i, 1 mM PP_i, 0.1 mM AMP, 3 mM AMPCPP, 14 mM $MgCl_2$, 100 mM NH_4Cl, and 100 mM imidazole (pH 6.9). No detectable exchange had taken place after a 1-h reaction period. The [^{14}C]AMP ⇄ ATP (methylenephosphonate) exchange reaction contained 1 unit/mL PPDK, 1.0 mM ATP, 1.0 mM AMP, 0.5 mM methylenephosphonate, 8 mM pyruvate, 14 mM MgCl, 100 mM NH_4Cl, and 100 mM PIPES (pH 7.0). After 2 h of incubation the reaction mixture contained no more [^{14}C]ATP than the control reaction (not containing methylenephosphonate) contained.

Discussion

The results of this study show that the *B. symbiosus* PPDK kinetic mechanism is bi bi uni uni (Scheme IV).[5] Three lines of evidence are presented in support of this mechanism. First, the initial velocity patterns observed for the ATP/P_i and AMP/PP_i pairs are intersecting, and the initial velocity patterns observed for the PEP/PP and PEP/AMP pairs are parallel (Table I). Second, PPDK was shown to catalyze [^{14}C]pyruvate ⇄ PEP exchange in the absence of the ATP/AMP and Pi/PP_i pairs, to catalyze [^{14}C]AMP ⇄ ATP only in the presence of the P_i/PP pair, and to catalyze [^{32}P]P_i

[5] Recent studies indicate that the *P. shermanii* PPDK also follows a bi bi uni uni mechanism (David Pocalyko and Debra Dunaway-Mariano, unpublished data).

$\rightleftarrows$ PP_i exchange only in the presence of the AMP/ATP pair (Table II). Third, PPDK catalyzes $\alpha\beta$-$^{18}O \rightarrow \alpha$-$^{18}O$ and β-$^{18}O \rightarrow \beta\gamma$-$^{18}O$ positional isotope exchanges in [$\alpha\beta$-^{18}O,β,β-$^{18}O_2$]ATP (**1**) and $\beta\gamma$-$^{18}O \rightarrow \beta$-^{18}O positional isotope exchange in [$\beta\gamma$-^{18}O,γ,γ,γ-$^{18}O_3$]ATP (**5**) in the presence but not in the absence of P_i (Figures 2 and 3, Table III).

The substrate binding order was investigated by carrying out dead-end inhibition studies in the case of the AMP/PP_i substrate pair (Table IV) and a combination of dead-end inhibition (Table IV), PIX (Figure 4), and alternate substrate studies in the case of the ATP/P_i substrate pair. The results obtained suggest that ATP and P_i binding is rapid equilibrium or steady state random and that AMP/PP_i binding is steady state ordered with AMP binding to the phosphoryl-enzyme before PP_i.

Product inhibition and equilibrium isotope exchange studies were carried out for the purpose of distinguishing between steady-state and rapid-equilibrium AMP/PP_i binding and for the purpose of identifying abortive complexes. Product inhibition of the forward reaction by PP_i was found to be noncompetitive vs ATP and vs P_i (Table V), which is consistent with the observed steady-state ordered addition of AMP and PP_i to EP. In addition, since PP_i binds to an enzyme form (EP·AMP) within the ATP $\rightleftarrows$ AMP exchange path, PP_i was expected to cause total inhibition of this exchange, which is found in the trend of the data shown in Figure 5C. Product inhibition of the forward reaction by AMP was found to be noncompetitive vs ATP and vs P_2. Since AMP binds to an enzyme form that, in the absence of PP_i, is not reversibly linked to the enzyme forms that ATP and P_i bind to, this inhibition should be uncompetitive. The noncompetitive inhibition that was observed suggests that AMP bind to E or E·P_i to form an abortive complex. To test for abortive complex formation, AMP inhibition[6] of the ATP $\rightleftarrows$ AMP and $P_i \rightleftarrows PP_i$ exchange reactions was measured. In both instances total inhibition was observed (Figure 5).

Product inhibition of the reverse reaction by ATP and P_i should be noncompetitive vs AMP and vs PP_i if ATP/P_i binding is steady state random but uncompetitive if ATP/P_i binding is rapid equilibrium random. In each instance noncompetitive binding was observed (Table V). This result is consistent with the steady-state mechanism but also can be accommodated by the rapid-equilibrium mechanism if abortive complex formation by ATP and P_i is assumed. For the purpose of testing for abortive complex formation by ATP and P_i the rate of the $P_i \rightleftarrows PP_i$ exchange reaction was measured as a function of the ATP and P_i concentration increased in constant ratio with the concentration of PP_i. As indicated in Figure 5, neither the ATP/PP_i nor the P_i/PP_i pair caused total inhibition of the $P_i \rightleftarrows PP_i$ exchange reaction. This result shows that the ATP/P_i binding steps are at steady state. The partial inhibition of the $P_i \rightleftarrows PP_i$ exchange reaction observed with the P_i/PP_i pair may reflect a preferred pathway involving initial ATP binding followed by P_i binding. The apparent downward curvature of the double-reciprocal plot of velocity vs ATP (or PP_i) shown in Figure 5 might also be indicative of preference for this pathway.

The kinetic data that we have presented for the *B. symbiosus* are clearly incompatible with the results and conclusions reported earlier (Milner et al., 1978). At the present time we cannot account for the discrepancy.[7] It is perhaps noteworthy

Scheme V

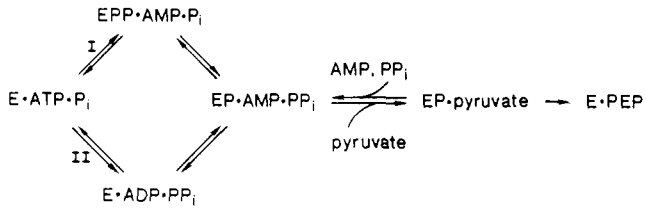

that the molecular isotope exchange data reported by Andrews and Hatch (1969) for the dikinase from sugar cane are consistent with data reported in this paper for the *B. symbiosus* enzyme. These workers concluded, as we have, in favor of a bi bi uni uni mechanism.

Revision of the PPDK kinetic mechanism from nonclassical tri uni uni to bi bi uni uni requires a reconsideration of the chemical mechanism of the reaction and the very unique catalytic mechanism of the enzyme proposed by Milner et al. (1978) and Milner and Wood (1976). There are two reasonable chemical mechanisms that one can consider for the PPDK reaction that are consistent with the bi bi uni uni kinetic mechanism, the known regiochemistry of the reaction (viz., ATP $\rightarrow PP_\gamma$, PEP_β, AMP_α) (Evans & Wood, 1968), and the known stereochemistry of the reaction (viz., inversion of configuration at the ATP γ-P and retention at the β-P) (Cook & Knowles, 1985). The first of these (Scheme V, mechanism I) is similar to that proposed by Milner et al. (1978) with the exception that P_i is necessary for pyrophosphorylation of the enzyme by ATP and that AMP release follows rather than precedes the reaction of the covalent pyrophosphoryl-enzyme with the P_i. The second mechanism (II) involves reaction of P_i and ATP to form ADP and PP_i. The ADP is not released from the enzyme but instead phosphorylates it, generating AMP.

According to mechanism I ATP α,β bond cleavage precedes β,γ bond cleavage while according to mechanism II ATP α,β bond cleavage follows β,γ bond cleavage. We therefore had hoped that a comparison of the $\alpha\beta \rightarrow \alpha$ PIX rate to the $\beta \rightarrow \beta\gamma$ PIX rate in [$\alpha\beta$-^{18}O,β,β-$^{18}O_2$]ATP (**1**) would allow us to distinguish between these two mechanisms. Unfortunately, the two PIX rates (Table III, Figure 4) were found to be equivalent, signifying that the first PIX reaction to occur is rate limiting. Thus, we were unable to make a distinction between the two mechanisms on the basis of these data.

Next, we turned to the use of substrate analogues to probe the β,γ and α,β bond cleavage steps. Adenylyl imidodiphosphate (AMPPNP) and adenylyl methylenediphosphate (AMPPCP) were shown to bind to the ATP binding site with high affinity [this work and Milner and Wood (1976)]. If α,β bond cleavage preceded β,γ bond cleavage, the possibility existed that PPDK could catalyze [^{14}C]AMP $\rightleftarrows$ AMPPNP or [^{14}C]AMP $\rightleftarrows$ AMPPCP exchange. We found that no exchange took place even when very high levels of enzyme were employed. This result could be a reflection of β,γ bond cleavage preceding, α,β bond cleavage, or it could simply reflect the differences in the chemical properties between ATP and the two analogues. Adenosine 5′-(α,β-methylenetriphosphate) (AMPCPP) was used to test for β,γ bond cleavage. PPDK was unable to catalyze [^{32}P]$P_i \rightleftarrows PP_i$ exchange in the presence of AMP/AMPCPP. Unfortunately, we do not know whether the failure of this exchange reaction to take place is a result of the operation of mechanism I or is simply a result of the difference between the chemical properties of ATP and AMPCPP. Lastly, we tested methylenephosphonate as a substitute for P_i in the [^{14}C]AMP $\rightleftarrows$ ATP exchange reaction. While methylenephosphoante is not a substrate for PPDK, the

[6] Although P_i and AMP were varied in constant ratio, P_i does not form a dead-end complex over the P_i concentration range used.

[7] Dr. Nelson Phillips has reported to us that he was unable to detect any significant ATP $\rightleftarrows$ AMP exchange reaction in the absence of P_i/PP_i.

possibility existed that it might function in the same manner that P_i would if mechanism I were operative. Again we found the substrate analogue unable to participate in the exchange reaction.

In conclusion, our studies show that *B. symbiosus* PPDK catalyzes two partial reactions: (1) ATP + P_i + E $\rightleftarrows$ AMP + PP_i + EP and (2) EP + pyruvate $\rightleftarrows$ E + PEP. The first partial reaction may proceed via a covalent pyrophosphoryl-enzyme intermediate as proposed earlier (Milner et al., 1978), or it may proceed via the intermediacy of ADP. At the present time studies that may allow us to distinguish between these possible chemical mechanisms are under way.

ACKNOWLEDGMENTS

We thank Drs. Nelson Phillips and Harland Wood for supplying us with their own *B. symbiosus* strain for comparison to the ATCC strain and for testing the ATP $\rightleftarrows$ AMP exchange reaction using PPDK prepared in our laboratory.

REFERENCES

Andrews, T. J., & Hatch, M. D. (1969) *Biochem. J. 114*, 117.
Benziman, M., & Palgi, A. (1970) *J. Bacteriol. 104*, 24.
Boyer, P. D. (1959) *Arch. Biochem. Biophys. 82*, 387.
Buchanan, G. (1974) *J. Bacteriol. 119*, 1066.
Cleland, W. W. (1979) *Methods Enzymol. 63*, 84.
Cohn, M., & Hu, A. (1978) *Proc. Natl. Acad. Sci. U.S.A. 75*, 203.
Cook, A. G., & Knowles, J. R. (1985) *Biochemistry 24*, 51.
Evans, H. J., & Wood, H. G. (1968) *Proc. Natl. Acad. Sci. U.S.A. 61*, 1448.
Goss, N. H., Evans, C. T., & Wood, H. G. (1980) *Biochemistry 19*, 5807.
Hanes, C. S., & Isherwood, F. A. (1949) *Nature (London) 164*, 1107.
Hatch, M. D., & Slack, C. R. (1968) *Biochem. J. 106*, 141.
Midelfort, C. F., & Rose, I. A. (1976) *J. Biol. Chem. 251*, 5881.
Milner, Y., & Wood, H. G. (1976) *J. Biol. Chem. 251*, 7920.
Milner, Y., Michaels, G., & Wood, H. G. (1978) *J. Biol. Chem. 253*, 878.
Moffatt, J. G., & Khorana, H. G. (1961) *J. Am. Chem. Soc. 83*, 649.
Phillips, N. F. B., & Wood, H. G. (1986) *Biochemistry 25*, 1644.
Radika, K., & Northrop, D. (1984) *Anal. Biochem. 141*, 413.
Reeves, R. E. (1960) *J. Biol. Chem. 243*, 3203.
Reeves, R. E., Munzies, R. A., & Hsu, D. S. (1968) *J. Biol. Chem. 243*, 5463.
Spronk, A. M., Yoshida, H., & Wood, H. G. (1976) *Proc. Natl. Acad. Sci. U.S.A. 73*, 4415.

Ristocetin-Dependent Reconstitution of Binding of von Willebrand Factor to Purified Human Platelet Membrane Glycoprotein Ib–IX Complex†

Michael C. Berndt,* Xiaoping Du, and William J. Booth
Research Centre for Thrombosis and Cardiovascular Disease, Department of Medicine, University of Sydney, Westmead Hospital, Westmead, NSW 2145, Australia

Received May 19, 1987; Revised Manuscript Received August 25, 1987

ABSTRACT: Whether the human platelet membrane glycoprotein (GP) Ib–IX complex is the receptor for ristocetin-dependent binding of von Willebrand factor (vWF) has been examined by reconstitution with the purified components using a solid-phase bead assay. Purified GP Ib-IX complex was bound and orientated on the beads via a monoclonal antibody, FMC 25, directed against the membrane-associated region of the complex. Specific binding of ^{125}I-labeled vWF to the GP Ib–IX complex coated beads was strictly ristocetin dependent with maximal binding occurring at ristocetin concentrations $\geq$1 mg/mL. Ristocetin-dependent specific binding of ^{125}I-labeled vWF was saturable. The observed binding was specific to the interaction between vWF and the GP Ib–IX complex since there was no ristocetin-dependent specific binding of vWF if the physicochemically related platelet membrane glycoprotein, GP IIb, was substituted for the GP Ib–IX complex in a corresponding bead assay. Further, neither bovine serum albumin nor other adhesive glycoproteins, such as fibrinogen or fibronectin, specifically bound to the GP Ib–IX complex in the presence of ristocetin. Ristocetin-dependent binding of vWF to platelets and to GP Ib–IX complex coated beads was inhibited by monoclonal antibodies against a 45 000 molecular weight N-terminal region of GP Ib but not by monoclonal antibodies directed against other regions of the GP Ib–IX complex. Similar correspondence between platelets and purified GP Ib–IX complex with respect to the ristocetin-dependent binding of vWF was obtained with anti-vWF monoclonal antibodies. The combined data indicate that the GP Ib–IX complex is the receptor involved in the ristocetin-dependent binding of vWF and that the specificity of this interaction is identical with that for the ristocetin-dependent binding of vWF to platelets.

The initial event in hemostasis in response to vascular injury involves the adhesion of platelets to the exposed subendothelial matrix. At high shear flow, the adhesion of platelets becomes von Willebrand factor (vWF)[1] dependent and involves a specific vWF receptor on the human platelet membrane (Chesterman & Berndt, 1986). In normal circulation, vWF does not bind to its platelet receptor. This interaction in vivo requires the prior binding of vWF to the subendothelial matrix

† This investigation was supported by Grant 6K14443 from the National Health and Medical Research Council of Australia. M.C.B. is the recipient of a Wellcome Australian Senior Research Fellowship.

[1] Abbreviations: EDAC, 1-ethyl-3-[3-(dimethylamino)propyl]carbodiimide hydrochloride; EDTA, ethylenediaminetetraacetic acid; GP, glycoprotein; SDS, sodium dodecyl sulfate; Tris, tris(hydroxymethyl)-aminomethane; vWF, von Willebrand factor.

0006-2960/88/0427-0633$01.50/0